CFD Analysis of Hull Separation and Vessel Speed on the Hydrodynamic Performance of Catamaran Trash Skimmers

Analiza utjecaja razmaka trupa i brzine plovila na hidrodinamičke performanse katamarana za prikupljanje otpada

Ahmad Firdhaus*
Diponegoro University
Faculty of Engineering
Department of Naval Architecture
Semarang, Indonesia
E-mail: afirdhaus@lecturer.undip.ac.id

Ahmad Fauzan Zakki
Diponegoro University
Faculty of Engineering
Department of Naval Architecture
Semarang, Indonesia
E-mail: ahmadfauzanzakki@lecturer.undip.ac.id

Samuel
Diponegoro University
Faculty of Engineering
Department of Naval Architecture
Semarang, Indonesia
E-mail: samuelaritonang@lecturer.undip.ac.id

Andi Trimulyono
Diponegoro University
Faculty of Engineering
Department of Naval Architecture
Semarang, Indonesia
E-mail: anditrimulyono@lecturer.undip.ac.id

Raichi Gumawan
Diponegoro University
Faculty of Engineering
Department of Naval Architecture
Semarang, Indonesia
E-mail: raiguwan654@gmail.com

DOI 10.17818/NM/2025/2.2
UDK 629.5.022.22:628.463
544.27
Original scientific paper / *Izvorni znanstveni rad*
Paper received / *Rukopis primljen:* 13. 1. 2025.
Paper accepted / *Rukopis prihvaćen:* 10. 6. 2025.

Abstract

Trash accumulation in water bodies necessitates efficient waste collection solutions, with catamaran-based trash skimmers offering a promising approach. However, their hydrodynamic performance in river conditions remains understudied. This research applies Computational Fluid Dynamics (CFD) modeling to assess how hull spacing and operational speed influence drag forces, fluid dynamics, and surface wave characteristics in restricted-depth aquatic environments. The results indicate that at lower speeds, hull separation has minimal impact on resistance, while at higher speeds, larger hull separation ratios (S/L) increase resistance due to wave interference and conveyor-induced disruptions. River conditions further amplify these effects, leading to increased drag and turbulence. These findings highlight the importance of optimizing hull spacing and speed to enhance hydrodynamic efficiency, particularly in confined environments, providing valuable insights for improving the design and operation of trash skimmer catamarans.

KEY WORDS

engineering
trash skimmer boat
catamaran
CFD
ship resistance

Sažetak

Nakupljanje otpada u vodama zahtijeva učinkovita rješenja za njegovo prikupljanje, pri čemu se katamarani za prikupljanje otpada čine obećavajućima. No, njihova hidrodinamička učinkovitost u riječnim uvjetima još uvijek nije dovoljno istražena. Ovo istraživanje primjenjuje modeliranje računalne dinamike fluida (CFD) kako bi se procijenio utjecaj razmaka između trupova i radne brzine na sile otpora, dinamiku fluida i karakteristike površinskih valova u vodenim okruženjima ograničene dubine. Rezultati pokazuju da pri manjim brzinama razmak između trupova ima minimalan utjecaj na otpor, dok pri većim brzinama veći omjeri razmaka trupa (S/L) povećavaju otpor zbog interferencije valova i poremećaja uzrokovanih transporterom. Riječni uvjeti dodatno pojačavaju ove učinke, dovodeći do povećanog otpora i turbulencije. Ovi nalazi ističu važnost optimizacije razmaka trupa i brzine plovila kako bi se poboljšala hidrodinamička učinkovitost, osobito u ograničenim okruženjima, pružajući korisne smjernice za unaprjeđenje dizajna i rada katamarana za prikupljanje otpada.

KLJUČNE RIJEČI

inženjerstvo
brod za prikupljanje otpada
katamaran
računalna dinamika fluida (CFD)
otpor broda

1. INTRODUCTION / *Uvod*

Over the past decade, the quantity of marine trash globally has markedly risen. The increase is attributable to direct ocean disposal, and 9% of trash originates from land through rivers and beaches [1,2]. Approximately 70% of marine debris is composed of plastic, totaling 390.7 million tons in weight as of 2021 [3]. This phenomenon is significant, particularly in light of the global output of plastic waste, which totals 407 million tons annually. Without robust preventive efforts, projections indicate that by 2050, the cumulative plastic trash generated may attain a staggering 33 billion tons [4].

Marine debris represents a substantial worldwide hazard to marine ecosystems and human health [5]. Numerous new solutions have arisen to tackle this problem, such as creating trash skimmer boats and autonomous vessels for debris collection [6,7]. These technologies employ sophisticated control systems and engineering methodologies to enhance

* Corresponding author

collecting efficiency [8]. Remote sensing methodologies are being investigated to assess marine trash [9]. Certain nations, such as Indonesia, are constructing specialist vessels for debris removal in small islands [10]. Virtual community centers are being built to improve collaboration and communication among stakeholders, facilitating knowledge sharing and public engagement in tackling the marine debris issue [11].

In response to the escalating issue of marine trash, numerous new concepts, techniques, and systems have been developed, including the Trash Skimmer Boat (marine debris collection vessel) [12]. Numerous research has been undertaken to optimize marine trash collection effectiveness across multiple dimensions. This encompasses an examination of the hull configurations on the Trash Skimmer Boat [13], revealing that the symmetrical trimaran model facilitates the collection of marine trash more effectively than the catamaran and monohull versions, as evidenced by the flow pattern characteristics at various speeds. In terms of resistance, the monohull type exhibits the least resistance as compared to the catamaran and symmetrical trimaran variants. Consequently, if the preferred model can efficiently collect trash with minimal resistance, the catamaran model can achieve both objectives. The simulation of catamaran hull form modifications [14] was conducted using models that include a symmetrical hull, an outside flat hull, and an interior flat hull, with differing distances between the hulls and the incorporation of a conveyor. The modeling findings indicate that the flat side outward (FSO) hull catamaran model possesses enhanced efficiency in trash collection. A literature assessment on the application of conveyors by Sugianto et al. [15] indicates that conveyors can be utilized in Trash Skimmer Boats at low speeds, as the vessel's speed is directly proportionate to the resistance encountered. Consequently, it is essential to analyze the fluctuations in the ship's hull distance and velocity to align with the operational objectives of the vessel [16–19].

Previous studies on the design of trash skimmer boats have not performed an analysis that reflects the original conditions. Consequently, the conceptual design for the hull shape of the trash skimmer boat utilizes a flat side outward (FSO) hull catamaran equipped with a conveyor between the demihulls, intended for operation in confined waters, representative of coastal and river environments. Efforts are undertaken to ensure optimal waste collection efficiency. Speed variations of 3 to 5 knots to ensure minimum operational ship resistance. This strategy aims for the Trash Skimmer Boat to serve as a more efficient and sustainable solution to the significant issue of marine waste while also positively contributing to the overall preservation of the maritime ecosystem. This study examines the impact of the distance between demi hulls on a trash skimmer catamaran operating in river conditions, specifically regarding ship resistance, flow contours, and wave height through variations in ship speed. This optimization relies on the ratio of the distance between the hulls in the Trash Skimmer Boat catamaran design. The simulation approach employs a numerical computing method grounded in computing Fluid Dynamics, specifically utilizing the free RANS (Reynolds Averaged Navier-Stokes) principle to analyze and describe intricate hydrodynamic forces.

2. MATERIALS AND METHODS / *Materijali i metode*

2.1. Research Object / *Predmet istraživanja*

The design used for the trash skimmer boat is a catamaran with a demi hull flat side outward (FSO) configuration. The main dimensions of this ship were obtained from previous research by Wulandari et al. [20]. Table 1 and Figure 1 display the principal dimensions of the ship and a 3D model of the trash skimmer boat, which serves as further supporting data.

Table 1 The main dimensions of the trash skimmer boat
Tablica 1. Glavne dimenzije broda za prikupljanje otpada

Main Dimension	Value
Length overall (LoA)	3 m
Length of water line (Lwl)	3 m
Breadth (B)	2 m
Height (H)	0,7 m
Draft (T)	0,29 m
Horsepower	6 HP
Conveyor angle	28°
Separation, S	0,9 m
Separation-to-length ratio, S/L	0,3

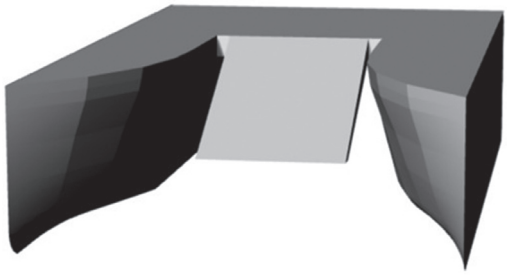

Figure 1 Trash skimmer boat 3D design
Slika 1. 3D prikaz broda za prikupljanje otpada

This investigation included altering the separation-to-length hull ratio and operational speed to determine optimal conditions for operating the trash skimmer boat. This research will replicate the operation of the trash skimmer boat in restricted water environments, such as beaches or rivers, to get results that closely resemble the actual operating circumstances. Table 2 presents the modifications and specifics of the setting to be developed in the present study.

Table 2 Variations in simulation conditions
Tablica 2. Varijacije u uvjetima simulacije

No	S/L	Water Depth (m)	Vs (knot)	Fr
1	0.2	2.15	3	0.28
2	0.3		4	0.38
3	0.4			
4	0.5		5	0.47

2.1. Numerical Approach / *Numerički pristup*

The governing equations for fluid flow are based on the principles of mass, momentum, and energy conservation. These fundamental equations form the foundation for the Reynolds-Averaged Navier-Stokes (RANS) approach used in this study to model turbulent flows. The mass conservation equation, also known as the continuity equation, ensures the incompressibility of the flow and is expressed as

$$\nabla \cdot U = 0 \quad (1)$$

Where U is the velocity vector, the momentum conservation equation describes the fluid's momentum exchange due to pressure, viscous forces, and turbulence, and it is given by the Reynolds-Averaged Navier-Stokes (RANS) equation:

$$\frac{\partial(\rho \mathrm{U})}{\partial t} + \nabla \cdot (\rho \mathrm{UU}) = -\nabla \mathrm{p} + \nabla \cdot (\mu(\nabla \mathrm{U} + (\nabla \mathrm{U})^T)) + F \quad (2)$$

Here, p is the pressure, μ is the dynamic viscosity, and F represents external forces. The computational fluid dynamics (CFD) software NUMECA was utilized to conduct the simulations with the turbulence model of $k-\omega$ Shear Stress Transport (SST). Several key equations form the basis of its calculations [21–24]. The transport equation for the turbulent kinetic energy (k), describes how turbulent kinetic energy changes over time, influenced by production, dissipation, and diffusion. This equation is expressed as follows:

$$\frac{\partial k}{\partial t} + U_j \frac{\partial k}{\partial x_j} = P_k - \beta^* \omega k + \frac{\partial}{\partial x_j}[(v + \sigma_k v_t)\frac{\partial k}{\partial x_j}] \quad (3)$$

Here, P_k Represents the production of turbulent kinetic energy, reflecting the transfer of energy from the main flow to turbulence. Meanwhile, $\beta^* \omega k$ represents the rate of dissipation of turbulent energy.

The second equation is the transport equation for the specific dissipation rate (ω), which also considers production, dissipation, and diffusion, with the addition of a particular function that allows the transition between the $k-\omega$ and $k-\varepsilon$ models:

$$\frac{\partial \omega}{\partial t} + U_j \frac{\partial \omega}{\partial x_j} = a\frac{\omega}{k} P_k - \beta\omega^2 + \frac{\partial}{\partial x_j}\left[(v + \sigma_\omega v_t)\frac{\partial \omega}{\partial x_j}\right] + 2(1 - F_1 \frac{\sigma_{\omega 2}}{\omega}\frac{\partial k}{\partial x_j}\frac{\partial \omega}{\partial x_j} \quad (4)$$

The function F_1 this equation plays a crucial role in the blending process between the characteristics of the $k-\omega$ and $k-\varepsilon$ models, allowing the $k-\omega$ SST model to handle various flow conditions more effectively.

Next, the turbulent viscosity (v_t) is calculated using the following relation:

$$v_t = \frac{a_1 k}{\max(a_1 \omega, SF_2)} \quad (5)$$

This relation ensures that the turbulent viscosity adaptively adjusts to the flow conditions, particularly in regions with high-velocity gradients.

Finally, the production of turbulent kinetic energy (P_k) is calculated as:

$$P_k = v_t(\frac{\partial U_i}{\partial x_j} + \frac{\partial U_j}{\partial x_i})\frac{\partial U_i}{\partial x_j} \quad (6)$$

This equation explains how energy from the main flow is transferred to turbulence through flow deformation.

The $k-\omega$ SST model, with these equations, enables more accurate flow simulations, especially in handling flow phenomena such as separation and reattachment [25]. The combination of the $k-\omega$ approach near walls and the $k-\varepsilon$ approach in the free stream region provides better predictive capabilities for pressure distribution and skin friction. Therefore, the use of the $k-\omega$ SST model in this study provides a solid foundation for analyzing complex turbulent flows [26].

In cases of multiphase flow, where the flow consists of two or more immiscible fluids (e.g., air and water), the Volume of Fluid (VOF) method is used to track the fluid interfaces. The VOF method tracks the volume fraction of each phase within each computational cell and is governed by the following equation.

$$\varepsilon = \left|\frac{f_1 - f_2}{f_1}\right| \times 100\% \quad (7)$$

Here, $\alpha_i \rho$ represents the volume fraction of phase i, ρ represents water density, and U represents the velocity vector. This method is essential for accurately capturing the behavior of phase interfaces, such as the free surface of water, in ship hull simulations.

In the context of space, the computational domain is partitioned into a set of control volumes, sometimes known as a mesh. Similarly, the time dimension is split into a limited number of discrete time steps [27]. The determination of timesteps is based on the recommendation of the ITTC standard formula [28] in equation (5), where L represents the ship's length overall (LOA) and U represents the ship's velocity. This yields timestep values in the range of $1.15\times10^{-3} - 1.98\times10^{-3}$, as shown in Table 3.

$$\frac{\partial(\alpha_i \rho)}{\partial t} + \nabla \cdot (\alpha_i \rho U) = 0 \quad (8)$$

Table 3 Timestep of each speed variation
Tablica 3. Vremenski korak za svaku varijaciju brzine

Fr	Knot	m/s	Δt
0.28	3	1.52	1.98×10^{-3}
0.38	4	2.06	1.46×10^{-3}
0.48	5	2.60	1.15×10^{-3}

2.1. Meshing and Boundary Condition / *Umrežavanje i granični uvjeti*

Figure 2 illustrates the computational domain's boundary conditions and meshing, following the ITTC guidelines [28]. The length of the domain extends from −2.5L to 1L, based on the length between perpendiculars (L), with the zero reference point located at the stern and draft of the vessel. The width was established as 1.5L, and the water depth was selected to simulate river conditions, resulting in a domain depth of 0.62L. The inlet, exit, and sidewall boundary conditions were uniformly assigned the same free-stream far-field velocity. The boundary conditions for the top wall were defined by a fixed pressure, while for the bottom wall, we applied a wall function to simulate the effects of river conditions. The ship surface was modeled with no-slip boundary conditions. For computational efficiency, the simulation was performed on only half of the hull. The normal velocity and gradient variables were set to zero at the symmetry plane condition.

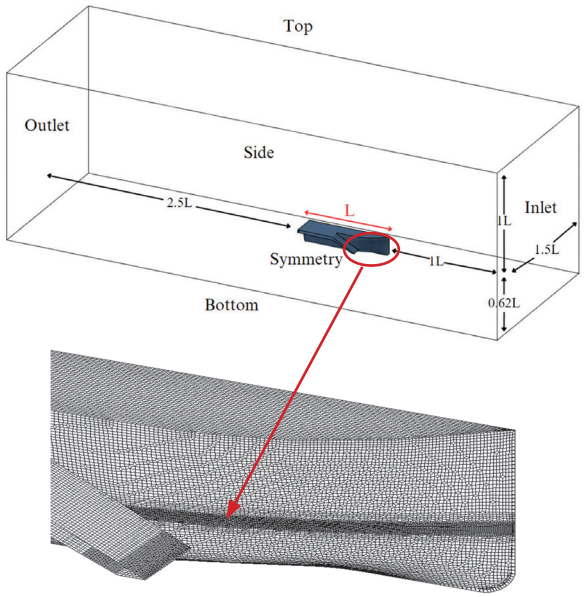

Figure 2 Boundary conditions and computational domain in conjunction with the simulation model
Slika 2. Granični uvjeti i računalna domena u kombinaciji sa simulacijskim modelom

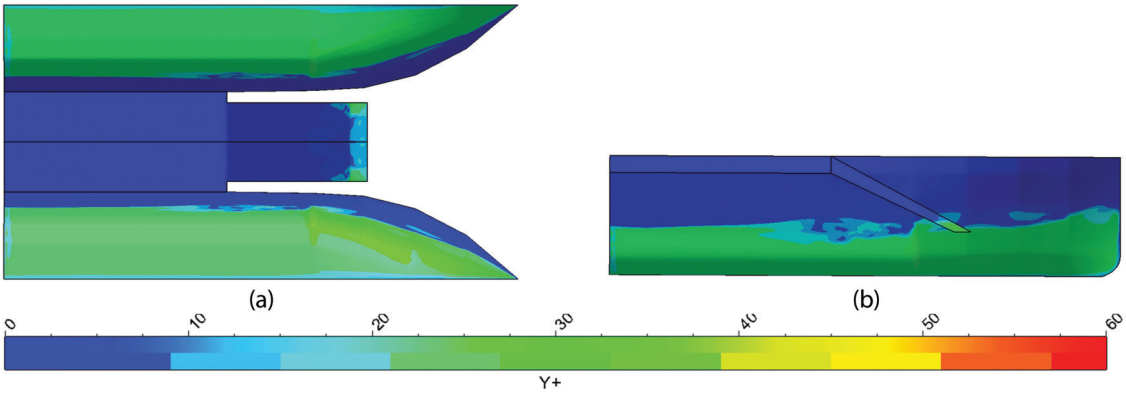

Figure 3 Wall Y+ on catamaran trash skimmer boat at Fr = 0.28 on (a) bottom view, (b) side view
Slika 3. Vrijednosti Y+ na katamaranu za prikupljanje otpada pri Fr = 0,28: (a) pogled odozdo, (b) bočni pogled

The simulation used an adaptive grid refinement technique to accurately resolve the air-water interface, which is crucial for analyzing wave dynamics. For real-time flow physics simulations, our method dynamically altered mesh resolution to prioritize directional refinement at the free surface to capture wave creation and propagation. The refinement procedure used flow-derived tensor fields to identify places requiring localized grid modifications, allowing targeted subdivision of cells along wave-aligned orientations and coarsening non-critical areas. This method precisely resolved transient wave heights and interface phenomena without refinement zones, decreasing computing costs.

The wall distance (Y+) is utilized in areas where the turbulence is significantly influenced by the viscosity of the wall. The dimensionless distance from the first grid node to the wall surface, Y+, is calculated using the local viscous length scale [25]. According to the 2011 International Towing Tank Conference (ITTC) guidelines, the Y+ value should fall within the range of 30–100 [25,29]. The calculation can be performed using the formula (6) as follows:

$$Y^{+} = \frac{U_{*}\gamma}{\upsilon} \tag{9}$$

Where U_{*} Represents the friction velocity at the closest wall, γ denotes the distance to the nearest wall, and υ signifies the local kinematic viscosity of the fluid. Figure 3 presents the Y+ value of the ship, which generally ranges between 20 and 40.

3. RESULTS AND DISCUSSIONS / *Rezultati i rasprava*

The results from the simulation in this study commenced with grid independence analysis to determine the mesh size that offers the most optimal computational cost, subsequently yielding data on total ship resistance, velocity contours, and wave elevation for each variation of the Trash Skimmer Boat catamaran design. The velocity contour results illustrate the fluid velocity in front of the conveyor to determine which demi hull distance facilitates a more rapid approach of the trash to the conveyor. Additionally, the flow pattern and wave height generated may be shown from the isosurface. Turbulent viscosity indicates the magnitude of the water vortex occurring in front of the conveyor; an immense vortex impedes the entry of trash into the conveyor. The ship speed variants are Fr 0.28, 0.38, and 0.48, with a demi hull distance (S/L) of 0.3 and variations of 0.2, 0.4, and 0.5.

3.1. Grid Independence / *Neovisnost mreže*

The Grid Independence test is performed to achieve an ideal equilibrium between total ship resistance and cell quantity, as seen in Figure 4. The numerical results were achieved using varying quantities of elements. The mesh was globally refined in successive iterations (e.g., coarse → medium →, fine) by uniformly reducing the base cell size across the domain while maintaining the structured topology. This approach ensures consistency in resolving flow features such as boundary layers, free-surface waves, and wake regions, which are critical for ship simulations. The disparity in the quantity of cell numbers is roughly 1.5 to 2 times more than the prior estimate [29]. This is attributable to the constraints of the computer processor used in the solver computation [26,30]. The methodology for the grid convergence index uses the error concept as delineated in Formula 7.

$$\Delta t = 0.001 \sim 0.01 \frac{L}{U} \tag{10}$$

Where ε denotes the relative approximation error between f_1(finer mesh) and f_2 (coarser mesh). Moreover, the error tolerance or variance between successive results is less than 10%. The grid independence analysis indicates that the ideal simulation of the Trash Skimmer Boat, conducted with 1.08×10^6 grids, exhibits a total drag force of 56.1 N at Fr 0.28, accompanied by an optimal resistance variation of 6%.

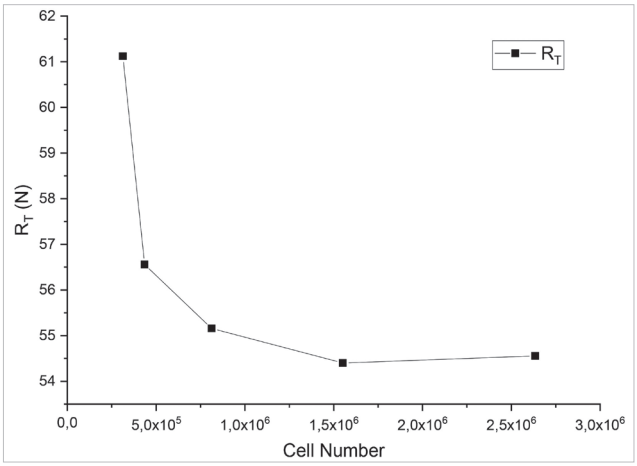

Figure 4 Graph of grid independence illustrating the relationship between cell number and ship resistance (R_T)
Slika 4. Grafikon neovisnosti mreže koji prikazuje odnos između broja ćelija i otpora broda (R_T)

3.2. Total Ship Resistance / *Ukupni otpor broda*

The investigation into the resistance of the trash skimmer catamaran was conducted using CFD models with varying distances between the hulls (S/L = 0.2, 0.3, 0.4, and 0.5). Figure 5 depicts the correlation between the force in the x-direction and the physical time of the simulation at 15 seconds. The catamaran simulation initiates with a distinct adjustment phase and thereafter stabilizes. Initially, the force

fluctuates rapidly as the flow surrounding the boat stabilizes into a pattern. Subsequent to this early phase, the fluctuations diminish significantly, resulting in a more level curve. At the conclusion of the graph, the line approaches a horizontal orientation, indicating that the force remains relatively constant over time.

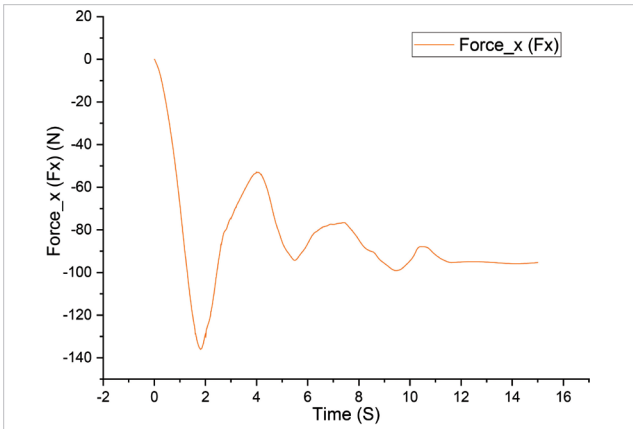

Figure 5 Force in the x direction (Fx) of CFD trash skimmer boat simulation at S/L 0.2, Fr 0.28 with the function of physical time simulation
Slika 5. Sila u x smjeru (Fx) pri S/L 0,2, Fr 0,28 s funkcijom vremenske simulacije u CFD prikazu broda za prikupljanje otpada

Figure 6 illustrates the relationship between the Froude number and the overall resistance of the vessel, where the Froude number quantifies the influence of vessel speed on resultant resistance. At low Froude numbers, changes in the distance between the demi hulls result in minimal variation in resistance outcomes, a finding consistent with previous research [31]. This indicates that hull separation has negligible influence on total resistance at lower speeds, as frictional resistance dominates the hydrodynamic profile under these conditions. At these speeds, frictional resistance is the dominant factor and is largely unaffected by the interaction between the hulls.

However, as the Froude number increases, a more noticeable difference emerges in resistance based on the demi hull spacing. Vessels with a more significant demi hull distance (S/L = 0.5) experience a more substantial increase in resistance compared to those with smaller spacings. Conversely, the model with an S/L ratio of 0.2 exhibits the least resistance as the Froude number grows. The resistance at higher speeds follows an order from highest to lowest based on the S/L ratio.

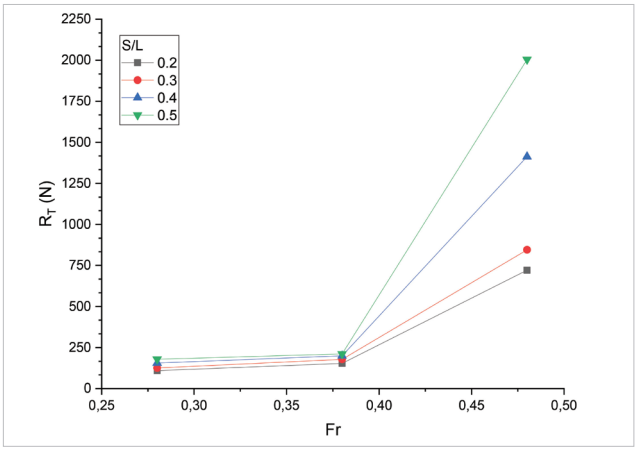

Figure 6 Total ship resistance (R_T) for all model variants as a function of the ship's Froude number
Slika 6. Ukupni otpor broda (R_T) za sve varijante modela kao funkcija Froudeova broja

Viscous and pressure forces contribute to ship resistance, as seen in Figure 7. The pressure force (FxP), measured at about 91.1 N, is the primary factor that determines the overall resistance of the catamaran at a Froude number of 0.28. The sum of the pressure and viscous components is measured at 95.3 N, which equals the total force (Fx). Although the force is small and inconsequential, the viscous force (FxV) is much less, contributing just 4.0 N. This effect suggests that, instead of frictional forces caused by the water's viscosity, the ship's hull encounters higher resistance due to pressure distribution on the surfaces.

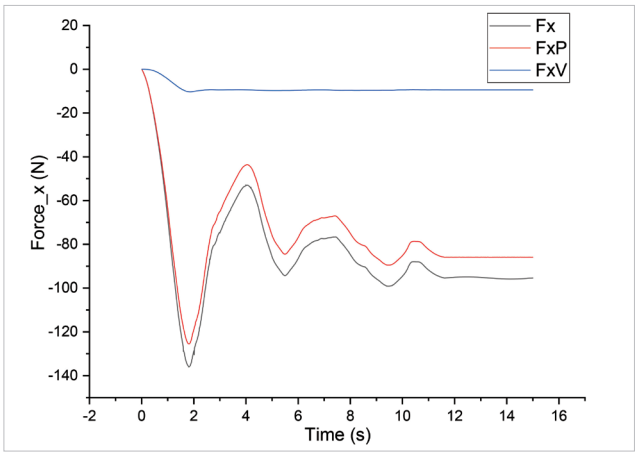

Figure 7 Resistance component of CFD simulation results of trash skimmer boat at Fr 0.28 at S/L 0.2
Slika 7. Sastavnice otpora prema rezultatima CFD simulacije broda za prikupljanje otpada pri Fr 0,28 i S/L 0,2

3.3. Velocity Contour / *Kontura brzine*

The simulation results of velocity contours on a trash skimmer boat equipped with a conveyor, conducted in a river condition domain, reveal hydrodynamic phenomena influenced by the ratio of the distance between the hulls (S/L) and the vessel's speed (Vs) are depicted in Figure 8. The river condition significantly affects the flow patterns, as the limited water depth amplifies the effects of total ship resistance, leading to stronger interactions between the flow and the hull surface, especially in the vicinity of the hull [32].

In the area around the hull, flow acceleration is observed, marked by a color gradient from green to yellow, indicating higher velocities of 2.0–3.0 m/s due to the flow interaction with the hull. However, within the space between the hulls, the relative velocity decreases, as shown by the color gradient from blue to green (0.5–1.5 m/s). This reduction in speed is mainly due to pressure buildup in front of the conveyor, which obstructs the flow path and causes deceleration in the demi hull region. In river conditions, this effect is more pronounced as the restricted water depth intensifies the deceleration and turbulence near the hull.

At lower S/L ratios (0.2 and 0.3), reduced hull separation enhances the Venturi effect, accelerating flow around the hulls and increasing wake turbulence behind the conveyor. This results in a more elongated and turbulent wake, leading to higher total ship resistance. Conversely, at higher S/L ratios (0.4 and 0.5), more significant hull separation reduces flow interactions between the hulls, promoting flow stability and a smaller, more uniform wake, which lowers resistance and improves hydrodynamic efficiency. The effect of this stabilizing flow pattern is more potent in river conditions due to the limited space for water movement between the hulls.

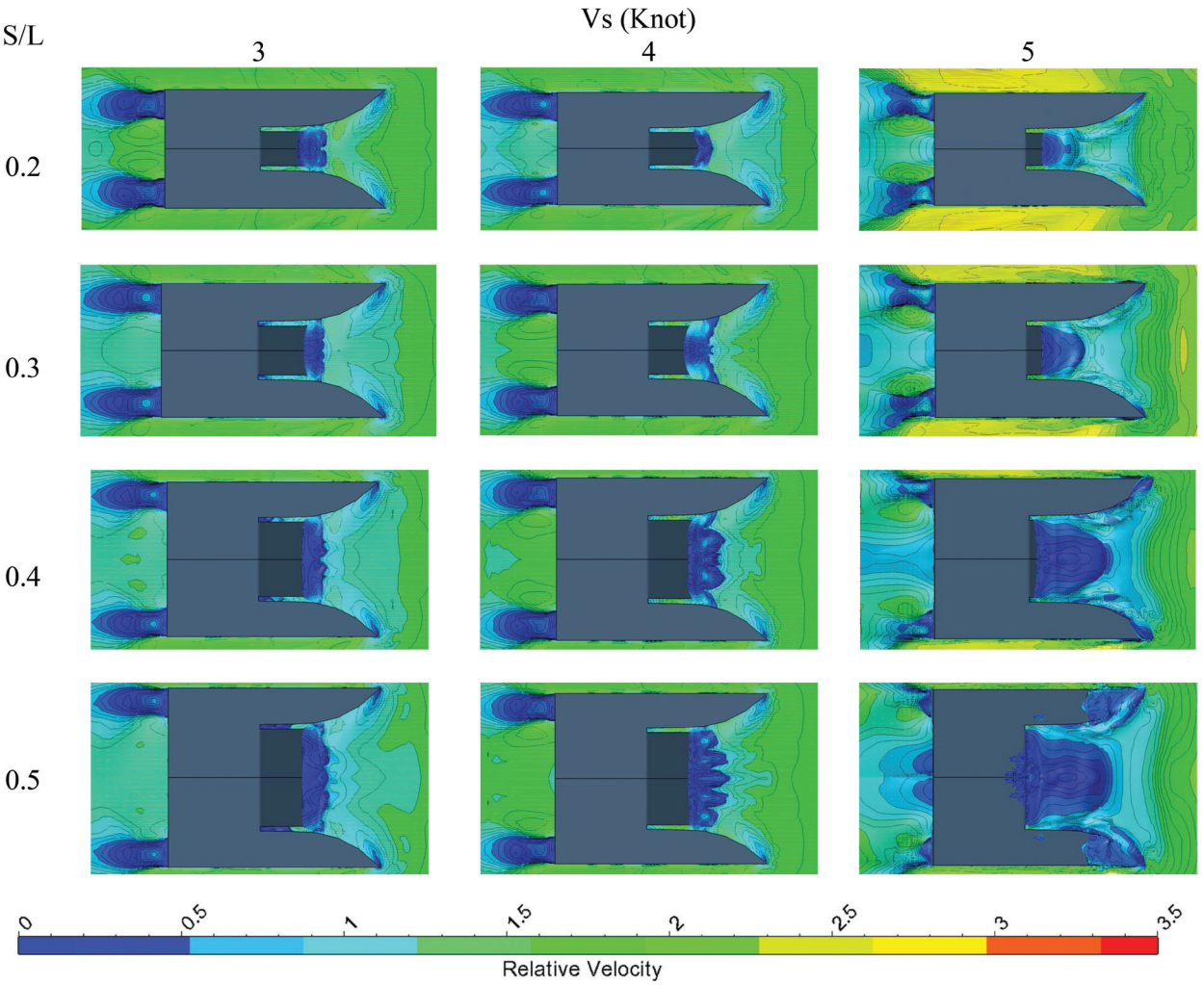

Figure 8 Visualization of velocity contour obtained through CFD simulation results of trash skimmer boat with S/L variations ranging from 0.2 to 0.4 at three distinct speeds: 3, 4, and 5 knots

Slika 8. Vizualizacija konture brzine dobivene rezultatima CFD simulacije broda za prikupljanje otpada s varijacijama S/L od 0,2 do 0,4 pri trima različitim brzinama: 3, 4 i 5 čvorova

The velocity contour patterns demonstrate that both the S/L ratio and vessel speed significantly affect flow behavior and total ship resistance in general. River conditions further amplify the effects of hull separation, as the confined space exacerbates flow deceleration and turbulence. A larger S/L ratio results in a more consistent flow, a smaller wake, and reduced resistance, while a smaller S/L ratio accelerates flow but increases turbulence and drag. The conveyor's presence, which obstructs the flow path between the hulls, increases deceleration, particularly at higher speeds and in river conditions. Therefore, optimizing the S/L ratio while considering the effects of river conditions is crucial for maximizing hydrodynamic efficiency, especially during high-speed operations, as it directly influences both flow dynamics and vessel performance.

3.4. Wave Elevation / *Visina valova*

The simulation results for the trash skimmer catamaran, equipped with a conveyor situated between the hulls, demonstrate the influence of varying speeds and hull spacing (S/L ratios of 0.2, 0.3, 0.4, and 0.5) on wave elevation, as seen in Figure 9. Conducted in a river condition domain, these simulations reveal how limited water depth can accentuate specific hydrodynamic effects, especially at higher speeds.

At lower speeds (3 and 4 knots), the wave patterns show minimal changes across different S/L ratios, with wave crests reaching up to 0.06 meters above the draft. This indicates that at these speeds, the conveyor's effect on wave elevation is negligible, and the vessel experiences a relatively constant flow with no significant variations in wave height due to hull spacing. The river conditions do not appear to alter these wave patterns significantly at lower speeds.

However, at higher speeds (5 knots), a significant increase in wave height is observed, with the maximum wave height reaching 0.26 meters over the ship's draft. At elevated velocities, the interaction between the water flow and the conveyor becomes more pronounced, leading to more substantial wave fluctuations and heightened turbulence. River conditions contribute to this effect by limiting the vertical space for wave formation, amplifying the intensity of the waves and turbulence near the hulls [33]. The wave patterns show a clear distinction between the areas before and after the conveyor, indicating increased energy dissipation and turbulent flow.

The impact of the S/L ratio becomes more pronounced at 5 knots. Smaller S/L ratios (0.2 and 0.3) produce larger wave amplitudes before the conveyor, while larger S/L ratios (0.4 and 0.5) result in more stable and uniform wave configurations. Despite these differences, the wave height remains significantly elevated at higher speeds, regardless of hull spacing, suggesting that the conveyor's flow disruptions become more prominent as speed increases. River

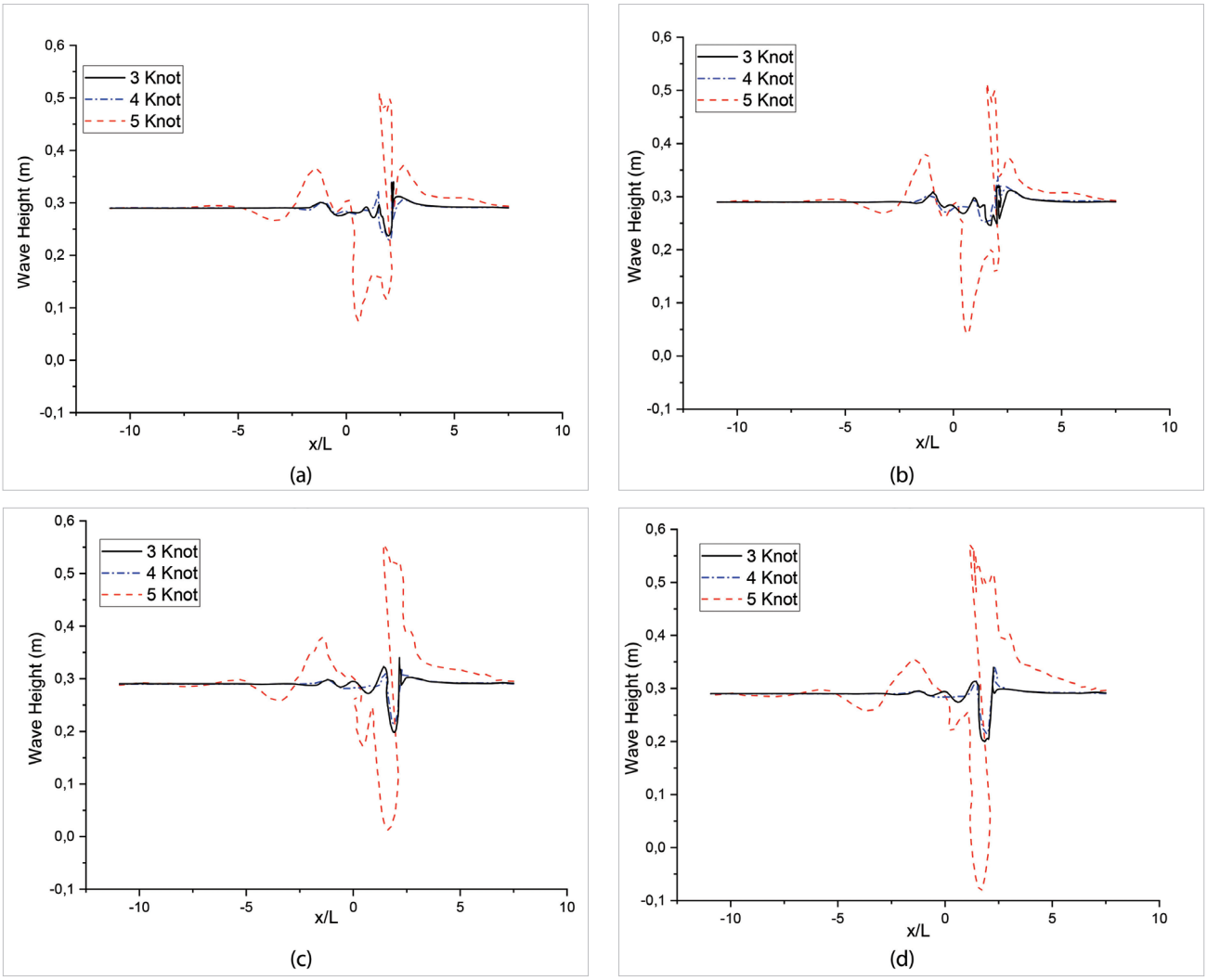

Figure 9 Wave elevation was determined by the CFD simulation results of the trash skimmer boat with S/L variation of (a) 0.2, (b) 0.3, (c) 0.4, and (d) 0.5

Slika 9. Visina valova određena je rezultatima CFD simulacije broda za prikupljanje otpada s varijacijama S/L od (a) 0,2, (b) 0,3, (c) 0,4 i (d) 0,5

conditions exacerbate these effects, as the restricted depth limits the flow dynamics and intensifies the wave patterns.

In summary, while changes in the S/L ratio have minimal effects on wave height at lower speeds, they become more significant at higher velocities, where increased hull separation stabilizes the waves. The presence of the conveyor between the hulls increases wave height and turbulence, particularly in river conditions, where the limited depth amplifies these effects. To optimize hydrodynamic efficiency, it is crucial to consider both vessel speed and proper hull spacing, especially in confined environments such as river conditions, where these factors are magnified.

5. CONCLUSIONS / *Zaključak*

Simulation of a trash skimmer catamaran equipped with a conveyor positioned between its hulls using CFD in river conditions, focusing on the impact of varying hull separation (S/L ratio 0.2, 0.3, 0.4, and 0.5) and vessel speed (3, 4, and 5 knots) has been successfully carried out. The simulation results on drag, flow pattern, wave height, and overall hydrodynamic efficiency.

At lower speeds (3 and 4 knots), changes in hull separation (S/L ratio) have minimal impact on resistance, flow patterns, and wave height. Frictional resistance dominates, and the hydrodynamic behavior of the vessel remains stable, regardless of hull separation. However, at higher speeds (5 knots), a significant increase in resistance and changes in flow patterns become more apparent, particularly with larger S/L ratios. Vessels with larger S/L ratios (0.4 and 0.5) experience a more substantial increase in resistance, likely due to greater energy loss from wave resistance and the disruptive effects of the conveyor. In river conditions, this effect is exacerbated by the confined space, further increasing drag and reducing the vessel's hydrodynamic efficiency.

The flow pattern simulations show that smaller S/L ratios (0.2 and 0.3) intensify the Venturi effect, accelerating the flow around the hulls but also increasing wake turbulence and drag. In contrast, larger S/L ratios (0.4 and 0.5) promote more stable flow, reducing wake turbulence and improving hydrodynamic efficiency, especially at higher speeds. In river conditions, the reduction in wake turbulence is more noticeable due to the limited depth at which the wake dissipates.

Wave elevation data further support these findings, showing that at lower speeds, the conveyor's influence on wave height is minimal, with wave peaks reaching only 0.06 meters. At 5 knots, the wave height increases significantly to 0.26 meters, with the greatest fluctuations occurring at lower S/L ratios. This suggests that at higher speeds, the conveyor's effect on flow disturbances, wave height, and turbulence is amplified, particularly in river conditions, where limited depth restricts the wave dissipation.

The significance of optimizing hull separation (S/L ratio) and vessel velocity to enhance the hydrodynamic efficiency of the trash skimmer catamaran, particularly at higher speeds in confined river environments, is emphasized. Reduced S/L ratios accelerate flow and increase drag, while larger S/L ratios stabilize flow and reduce turbulence. The conveyor has a significant impact on wave height and resistance, particularly at higher speeds, making it crucial to balance hull spacing and operational velocity. Moreover, accurate CFD modeling of the conveyor is essential to replicate real-world flow conditions, ensuring that the simulation results align closely with actual vessel performance. Proper modeling of the conveyor's shape, flow interactions, and its effects on the water flow in the demi hull region guarantees more reliable data for optimizing the design and enhancing operational efficiency.

This study offers significant insights into the hydrodynamic performance of a trash skimmer catamaran in river conditions; however, it is constrained by idealized CFD simulations that presume steady flow and simplified conveyor geometry, potentially failing to encompass intricate real-world phenomena such as transient currents, sediment transport, and debris accumulation. The study was confined to certain hull separations and vessel speeds, hence restricting the examination of continuous parameter ranges and other operational aspects like load fluctuations and maneuvering impacts. Future research must concentrate on integrating transient and unstable river flow conditions, testing simulations against experimental or field data, and enhancing conveyor models via intricate geometry and dynamic components to more accurately emulate real flow interactions.

Author Contribution: Research, A. F., A. F. Z., and R. G.; Data collection, R. G.; Formal analyses, A. F. and R. G.; Writing, A. F.; Review and editing, S. and A. T.; Supervision, A. F. Z., Final approval, A. F. Z.

Funding: This research was financially supported by The Faculty of Engineering, Diponegoro University, Indonesia, through International Collaboration Research Grant 2024

Conflict of interest: None

Acknowledgments: The authors would like to convey their appreciation to The Faculty of Engineering, Diponegoro University, Indonesia for funding this research through International Collaboration Research Grant 2024

REFERENCES / *Literatura*

[1] Naidoo, T., Rajkaran A., & Sershen (2020). Impacts of plastic debris on biota and implications for human health: A South African perspective. *South African Journal of Science*, *116* (5/6). https://doi.org/10.17159/sajs.2020/7693

[2] Sánchez-Ferrer, A., Valero-Mas, J. J., Gallego A. J., & Calvo-Zaragoza J. (2023). An experimental study on marine debris location and recognition using object detection. *Pattern Recognition Lette*rs, 168, 154-161. https://doi.org/10.1016/j.patrec.2022.12.019

[3] van Emmerik T., & Schwarz A. (2020). Plastic debris in rivers. *WIREs Water*, *7* (1). https://doi.org/10.1002/wat2.1398

[4] Haque MdK, Uddin M., Kormoker T. et al. (2023). Occurrences, sources, fate and impacts of plastic on aquatic organisms and human health in global perspectives: What Bangladesh can do in future?. *Environmental Geochemistry and Health*, *45* (8), 5531-5556. https://doi.org/10.1007/s10653-023-01646-0

[5] Agamuthu P., Mehran S., Norkhairah A., & Norkhairiyah A. (2019). Marine debris: A review of impacts and global initiatives. *Waste Management & Research*, *37* (10), 987-1002. https://doi.org/10.1177/0734242X19845041

[6] Rafi, M., Hanafi R., & Santoso D. T. (2021). Design and Build a Trash Skimmer Boat as a Solution For Collecting Trash in Indonesian Rivers. *Journal of Mechanical Engineering Manufactures Materials and Energy*, *5* (1), 57-68. https://doi.org/10.31289/jmemme.v5i1.4402

[7] Kong, Q. (2024). Autonomous Vessel Design for Efficient Marine Debris Collection: A MATLAB Simulink and Arduino-Based Approach. *Science and Technology of Engineering, Chemistry, and Environmental Protection*, *1* (5). https://doi.org/10.61173/qcxhmx26

[8] Jung, R. T., Sung, H. G., Chun, T. B., & Keel, S. I. (2010). Practical engineering approaches and infrastructure to address the problem of marine debris in Korea. *Marine Pollution Bulletin*, *60* (9), 1523-1532. https://doi.org/10.1016/j.marpolbul.2010.04.016

[9] Moller, D., Chao, Y., & Maximenko, N. (2016). Remote sensing of marine debris. In: *IEEE International Geoscience and Remote Sensing Symposium (IGARSS)*, 7690-7693. https://doi.org/10.1109/IGARSS.2016.7731005

[10] Chandra, H., Rahmania, R., Kusumaningrum, P. D. et al. (2021). Developing the Debris Incinerator Vessel as a New Solution for Managing Marine Debris in Small Islands of Indonesia. *IOP Conference Series: Earth and Environmental Science*, *925* (1), 012016. https://doi.org/10.1088/1755-1315/925/1/012016

[11] Plag, H. P., Jones, K., Garello, R. (2021). A Virtual Center for the Community Addressing the Challenge of Marine Debris. In: *OCEANS 2021: San Diego – Porto*. *IEEE*, 2021-8. https://doi.org/10.23919/OCEANS44145.2021.9705762

[12] Sugianto, E., Chen, J. H., & Purba, N. P. (2023). Cleaning technology for marine debris: A review of current status and evaluation. *International Journal of Environmental Science and Technology*, *20* (4), 4549-4568. https://doi.org/10.1007/s13762-022-04373-8

[13] Sugianto, E., Winarno, A., Indriyani, R., & Chen, J. H. Kapal (2021). Jurnal Ilmu Pengetahuan dan Teknologi Kelautan Hull Number Effect in Ship Using Conveyor on Ocean Waste collection t) Check for. *Jurnal Ilmu Pengetahuan dan Teknologi Kelautan*, *18* (3), 128-139. https://doi.org/10.14710/kapal.v18i3.40744

[14] Sugianto, E., Zamzami, R. A., Winarno, A., & Prasutiyon, H. (2023). Effect of catamaran hull type on ocean waste collection behavior. *Journal of Marine-Earth Science and Technology*, *3* (3), 79-85. https://doi.org/10.12962/j27745449.v3i3.590

[15] Sugianto, E., Horng-Chen, J., & Purba, N. P. (2021). Numerical investigation of conveyor wing shape type effect on ocean waste collection behavior. *E3S Web of Conferences*, 324, 01005. https://doi.org/10.1051/e3sconf/202132401005

[16] 1Firdhaus, A., Kiryanto, K., Rindo, G., & Trimulyono, A. (2024). Analysis of Interference Factor in Hydrofoil-Supported Catamarans (HYSUCAT). *Kapal: Jurnal Ilmu Pengetahuan dan Teknologi Kelautan*, *21* (1), 1-9. https://doi.org/https://doi.org/10.14710/kapal.v21i1.61750

[17] Firdhaus, A., Kiryanto, Hakim, M. L., Rindo, G., & Iqbal, M. (2024). Ship Performances CFD Analysis of Hydrofoil-Supported High-Speed Catamaran Hull Form. *Journal of Advanced Research in Fluid Mechanics and Thermal Sciences*, *113* (1), 108-121. https://doi.org/10.37934/arfmts.113.1.108121

[18] Firdhaus, A. & Suastika, I.K. (2022). Experimental and Numerical Study of Effects of the Application of Hydrofoil on Catamaran Ship Resistance. In: *The International Conference on Marine Technology (SENTA)*. *Scitepress*, 104-110. https://doi.org/10.5220/0010854400003261

[19] Utama, IKAP, Sulisetyono, A., Ali B. et al. (2024). Seakeeping Performance of Warship Catamaran under Varied Hull Separation and Wave Heading Conditions. *Pomorstvo*, *38* (2), 275-296. https://doi.org/10.31217/p.38.2.9

[20] Wulandari, A. I., Setiawan, W., Hidayat, T., & Fauzi, D. A. (2020). Design of Trash Skimmer Boat for Inland Waterways in East Kalimantan. *Wave: Jurnal Ilmiah Teknologi Maritim*, 14, 9-18. https://doi.org/10.29122/jurnalwave.v14i1.4087

[21] Menter, F. R.(1994). Two-equation eddy-viscosity turbulence models for engineering applications. *AIAA Journal*, *32* (8), 1598-1605. https://doi.org/10.2514/3.12149

[22] Menter, F. R. (1992). Influence of free-stream values on k-omega turbulence model predictions. *AIAA Journal*, *30* (6), 1657-1659. https://doi.org/10.2514/3.11115

[23] Menter, F. R. (1993). Zonal Two Equation k-w Turbulence Models For Aerodynamic Flows. In: *23rd Fluid Dynamics, Plasmadynamics, and Lasers Conference. Fluid Dynamics and Co-located Conferences. American Institute of Aeronautics and Astronautics*. https://doi.org/10.2514/6.1993-2906

[24] Menter, F. R. (1992). Performance of popular turbulence model for attached and separated adverse pressure gradient flows. *AIAA Journal*, *30* (8), 2066-2072. https://doi.org/10.2514/3.11180

[25] Yonatan, Y., Darma, E., Hendra Pratama, R., Satria, IGNA, Dharma Yudha, P., & Kusuma A. I.(2024). Impact of Stepped Hull Design on Speed Boat Performance: A CFD Study. *EVERGREEN Joint Journal of Novel Carbon Resource Sciences & Green Asia Strategy*. 11, 2580-2589. https://doi.org/10.5109/7236898

[26] Vassberg, J. C., & Jameson, A. (2010). Pursuit of Grid Convergence for Two-Dimensional Euler Solutions. *Journal of Aircraft*., *47* (4), 1152-1166. https://doi.org/10.2514/1.46737

[27] Zafirah, N., Bakar, A., & Padzillah, M. H. (2024). Comparison between Computational Fluid Dynamics and Fluid-Structure Interaction Models of an Automotive Mixed Flow Turbocharger Turbine. *EVERGREEN Joint Journal of Novel Carbon Resource Sciences & Green Asia Strategy*, 11, 1457-1470. https://doi.org/10.5109/7183474

[28] ITTC (2014). *Recommended Procedures and Guidelines Practical Guidelines for Ship Resistance CFD.*

[29] Anderson, J. (1995). *Computational Fluid Dynamics; The Basic With Applications*.

[30] Lee, M., Park, G., Park, C., & Kim, C.(2020). Improvement of Grid Independence Test for Computational Fluid Dynamics Model of Building Based on Grid Resolution. *Advances in Civil Engineering*, 1. https://doi.org/10.2514/1.4673710.1155/2020/8827936

[31] Yanuar, I., Karim, S., & Ichsan, M. (2017). Experimental study of the interference resistance of pentamaran asymmetric side-hull configurations. In: *AIP Conference Proceedings*, 1826. https://doi.org/10.2514/1.4673710.1063/1.4979241

[32] Hoa, N. T. N., Bich, V. N., Tu, T. N., Chien, N. M., & Hien, L. T. (2019). Numerical Investigating the Effect of Water Depth on Ship Resistance Using RANS CFD Method. *Polish Maritime Research*, *26* (3), 56-64. https://doi.org/10.2514/1.4673710.2478/pomr-2019-0046

[33] Fenton, J. D., Huber, B., Klasz, G., & Krouzecky, N. (2023). Ship waves in rivers: Environmental criteria and analysis methods for measurements. *River Research and Applications*, *39* (4), 629-647. https://doi.org/10.1002/rra.4101